Physics and Imaging in Radiation Oncology 19 (2021) 78–84

Contents lists available at ScienceDirect

Physics and Imaging in Radiation Oncology

journal homepage: www.sciencedirect.com/journal/physics-and-imaging-in-radiation-oncology

A proof of concept treatment planning study of gated proton radiotherapy for cardiac soft tissue sarcoma

Hyeri Lee [*,1], Jennifer Pursley, Hsiao-Ming Lu [2], Judith Adams, Thomas DeLaney, Yen-Lin Chen [3], Kyung-Wook Jee [3]

Department of Radiation Oncology, Massachusetts General Hospital and Harvard, Medical School, Boston, MA 02114, USA

ARTICLE INFO

Keywords:
Proton therapy
Cardiac irradiation
Cardiac gating
Cardiac dose reduction

ABSTRACT

Background and Purpose: Few studies on radiotherapy of cardiac targets exist, and none using a gating method according to cardiac movement. This study aimed to evaluate the dose-volume advantage of using cardiac-respiratory double gating (CRDG) in terms of target location with additional ECG signals in comparison to respiratory single gating (RSG) for proton radiotherapy of targets in the heart.

Materials and Methods: Cardiac motion was modeled using a cardiac-gated four-dimensional computed tomography scan obtained at the end-expiration. Plans with the prescription dose of 50 Gy (RSG and CRDG plans at diastole and systole phases) were compared in terms of clinically relevant dose-volume criteria for various target sizes and seven cardiac subsites. Potential dose sparing by utilizing CRDG over RSG was quantified in terms of surrounding organ at risk (OAR) doses while the dose coverage to the targets was fully ensured.

Results: The average mean dose reductions were 28 ± 10% when gated at diastole and 21 ± 12% at systole in heart and 30 ± 17% at diastole and 8 ± 9% at systole in left ventricle compared to respiratory single gating. The diastole phase was optimal for gated treatments for all target locations except right ventricle and interventricular septum. The right ventricle target was best treated at the systole phase. However, an optimal gating phase for the interventricular septum target could not be determined.

Conclusions: We have studied the dose-volume benefits of CRDG for each cardiac subsite, and demonstrated that CRDG may spare organs at risk better than RSG.

1. Introduction

Primary cardiac soft tissue sarcoma is an extremely rare and aggressive malignancy with a prevalence estimated at only less than 0.03%, with a median survival of less than one year [1–5]. The majority of these malignancies originate from atria but they can also be found in other cardiac subsites including the interventricular septum or heart valves. The primary treatment has been open surgical resection; the role of chemo- and radiation therapy is not yet well-understood because of the limited number of cases treated with those modalities [5]. A recent multi-institutional retrospective study from the French Sarcoma Group showed that radiation therapy was associated with improved progression-free survival, using photon techniques [6,7]. For proton and heavy-ion therapies, even fewer cases have been reported on [8,9].

Radiation treatment of a cardiac target is challenging, complicated not only by the respiratory motion but also by the cardiac contractile motion and the interplay between these two motions. The cycle of the cardiac motion is shorter, less than a second compared to several seconds for a respiratory cycle. These make tracking a cardiac target and mitigating its motion challenging for delivery of radiotherapy. In the case of treatment sites affected only by respiration-induced organ motion, various techniques successfully mitigate the motion with various strategies such as respiratory gating, or a use of expanded target volume called *internal target volume* (ITV) [10]. Recent studies for cardiac irradiation have been mainly focused on catheter-free ablation for cardiac arrhythmia such as atrial fibrillation and ventricular tachycardia [11–17], although cardiac irradiation of primary cardiac sarcoma has been around for many years [5–8]. The catheter-free approach has

* Corresponding author at: Radiation Oncology, Massachusetts General Hospital, 55 Fruit Street, Lunder Building, LL 236, Boston, MA 02114, USA.
E-mail address: Hyeri.Lee@osumc.edu (H. Lee).
[1] Present address: Ohio State University, Wexner Medical Center, James Cancer Hospital in Columbus, OH, USA.
[2] Present address: Hefei Particle Therapy Center in Hefei, China.
[3] Co-senior authors with equal contributions made in the conceptualization, oversight, design, guidance, and analysis of the results of the study.

https://doi.org/10.1016/j.phro.2021.06.001
Received 19 November 2020; Received in revised form 23 May 2021; Accepted 3 June 2021

attracted attention and also evoked concerns related to the efficacy and safety of cardiac irradiation [11]. However, research on the dose-volume impact of cardiac motion has been limited [16,18], or only in animals [15,17].

In radiation therapy settings, the target motion for cardiac sarcoma patients is accounted for with an ITV, while the treatment is delivered with respiratory gating [19,20] or without respiratory gating [6,7,9,11]. While this ensures that the entire motion of the target is included, if a treatment beam could be delivered at a particular cardiac phase with additional cardiac gating, the treatment volume can potentially be further reduced, leading to further sparing of surrounding organs at risk (OAR) and normal tissues.

The aim of this study was to evaluate the potential dose-volume advantages of using cardiac gating with ECG as well as respiratory gating – a technique here referred as cardiac-respiratory double gating (CRDG). We compared the dose-volume benefits of CRDG over Respiratory Single Gating (RSG) to further reduce OAR doses.

2. Materials and methods

In this article, RSG refers to respiratory single gating using the average intensity projection of cardiac 4D CT, while CRDG refers to the ECG-gated technique; both techniques employ exhale respiratory gating.

2.1. Images and target delineation

Multiple targets were defined and studied based on a single patient subject in order to evaluate the dose-volume effects of target locations exclusive of patient-specific anatomical variations. The patient was female and diagnosed with malignant neoplasm of heart at the age of 41, and the cancer was located in mediastinum. For the study subject, a time-resolved cardiac four-dimensional (4D) computed tomography (CT) was obtained on Siemens Somatom Force CT scanner (Siemens Healthcare GmbH, Erlangen, Germany) with contrast. The cardiac CT acquisition was made at the end of exhale. The CT slices were sorted retrospectively using a cardiac gating signal (i.e., ECG) into 10 motion phases of a RR interval for a cardiac cycle (Supplementary Material Fig. 1). Diastole was at 0% of RR interval of cardiac cycle and Systole was at 40% for this scan, where the RR interval is the time between successive heartbeats. All images were reconstructed at 1 mm slice thickness with 255 slices. The image resolution was 512×512, and the voxel size was (1.0×1.0) mm^2. Cardiac substructures such as Left Atrium, Left Ventricle, Left Ventricular Free Wall, Right Atrium, Right Atrial Free Wall, Right Ventricle, right coronary artery (RCA), left anterior descending artery (LAD) and mitral valve and surrounding OARs were contoured. The study was institutional review board approved. For this non-interventional planning study, ethics approval was not needed. Seven mock targets located at various cardiac substructures were also contoured using MiM (MiM Software Inc., Cleveland, OH) by an expert radiation oncologist.

2.2. Treatment planning

Treatment planning was performed in the proton XiO planning system (Elekta, Stockholm, Sweden) with an in-house developed pencil beam algorithm for the dose calculation [21]. For both planning and dose calculation, the HU values of contrast enhanced areas in CTs were overwritten with a generic density (HU = 50). For each target location, two CRDG plans were generated, one for a double-gated treatment at the diastole phase of the cardiac cycle and the other at the systole phase. RSG targets included a cardiac ITV combined from all 10 cardiac phases and were planned on the average intensity projection of cardiac 4DCT. Once RSG plans were made from the average intensity projection CT, the beams were then applied to each of the 10 cardiac phase CTs, resulting in 10 dose distributions which were then accumulated onto a reference phase CT using the deformable registration workflow in MiM to simulate the actual 4D dose distribution. Dose-Volume Histograms (DVHs) were calculated in MiM.

2.3. Dose comparison

The PTV volumes were prescribed to a nominal prescription dose of 50 Gy and PTV coverage of $V_{95} \geq 95\%$ prescribed dose was required for all treatment plans. The plan quality comparison was therefore in *iso*-benefit, meaning that all plans provide a reasonable target coverage and the plan quality differences were assessed only in terms of dose sparing to OARs and normal tissues. All plans were generated for double scattered proton beam deliveries with the following planning parameters: an aperture margin of 1 cm, a range compensator smearing of 0.5 cm, and a range margin of 3.5% accounting for range uncertainty.

OAR dose sparing was analyzed with the dose limits of OARs listed in Supplementary Material Table 1 [22–24]. The normal heart is defined as the whole heart excluding the target volume. The percent reduction was calculated as a ratio of the mean dose (MD) differences between RSG plans and each CRDG plan to the mean OAR dose at RSG plans $\left(\frac{MD(RSG)-MD(CRDG)}{MD(RSG)}\right)$.

Dose coverages of targets were quantified with three dose-volume criteria, i.e., dose homogeneity (D_5–D_{95}) which is the dose difference covering 5% and 95% of the target volume, dose coverage V_{95}, and V_{107} (volume receiving $\geq$ 107% prescribed dose) assessing the overdose.

Due to the absence of exit dose with protons, OAR doses are largely dependent on the orientation of incoming proton beams. The proximity of surrounding OARs normally constrains the proton beam arrangement; however, there is generally a trade-off between target coverage and OAR sparing. To evaluate this trade-off relationship, a total of 29 plans with 26 beam angles were first generated at a diastole phase, where each incoming beam angle decides an aperture and a range compensator. We also analyzed the relationship between the dose homogeneity (D_5–D_{95}) and the beam range (where the range is defined and determined by the water-equivalent thickness to the distal-end of the target).

2.4. Target motion analysis

The residual motions were calculated for 20, 30 and 40% duty cycles for each gating phase. The displacements were the distances between the center of PTVs. The volume changes were quantified in terms of absolute (mL) and relative volume (%).

3. Results

For a total of seven plans with three modes, PTV volumes varied from 2.5 cm^3 to 201.8 cm^3 (median, 86.4 cm^3). The median volume reduction from the RSG targets to the CRDG targets in diastole and systole was 21.7 cm^3 and 23.3 cm^3, respectively (Supplementary Material Table 2). PTV_{95} (%) was 99.6 ± 0.9, V_{107} (%) was 0.0 ± 0.1 and D_5–D_{95} (Gy) was 1.8 ± 0.7, presented in Supplementary Material Table 3. The RSG plans irradiated larger cardiac volumes compared to CRDG plans due to the need to cover an ITV including all motions in a cardiac cycle (Fig. 1).

All OAR metrics met the planning constraints explicitly (Fig. 2). Median mean doses for the esophagus and lungs were 0.15 Gy and 3.5 Gy, respectively. The median mean doses to cardiac structures (heart, left ventricle, RCA, and LAD) were 12.4 Gy, 11.5 Gy, 7.8 Gy, and 3.7 Gy for all plan configurations, respectively.

The considered beam angles for each target are listed in Supplementary Material Table 4. The strong dependence of target coverage and OAR dose on beam angle is illustrated in Fig. 3A using an example target located at LVFW while adequate coverage was ensured. All field arrangements provided adequate target coverage (V_{95}) and clinically acceptable hotspots (V_{107}) among the target dose metrics (Fig. 3B). For a choice of beam angle, the homogeneity varied between 1.9 Gy and 5.2 Gy and the hotspots ranged from 0 to 3%. Fig. 3C presents trade-offs in

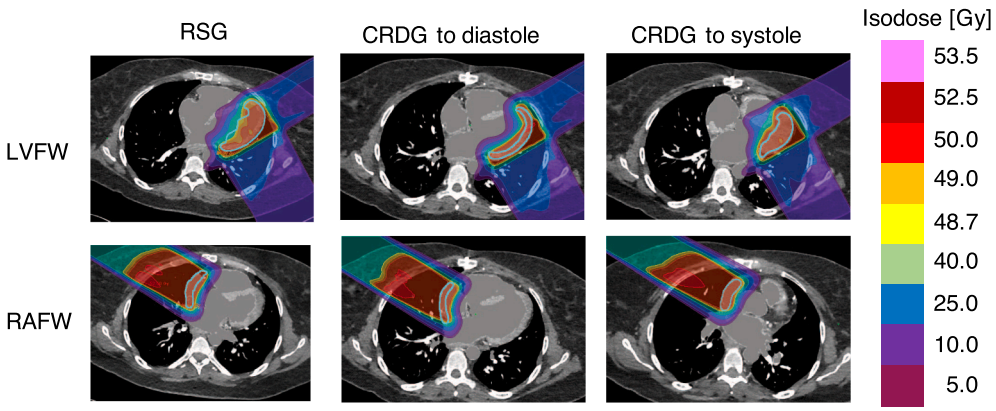

Fig. 1. Dose distribution (transverse view) comparing RSG (left) and CRDG plans (diastole (middle) and systole (right)) for two targets (Left ventricular free wall (LVFW, top) and Right atrium free wall (RAFW, bottom)). The contoured targets are presented as a solid light blue line. Isodose levels are shown on the right. (For interpretation of the references to colour in this figure legend, the reader is referred to the web version of this article.)

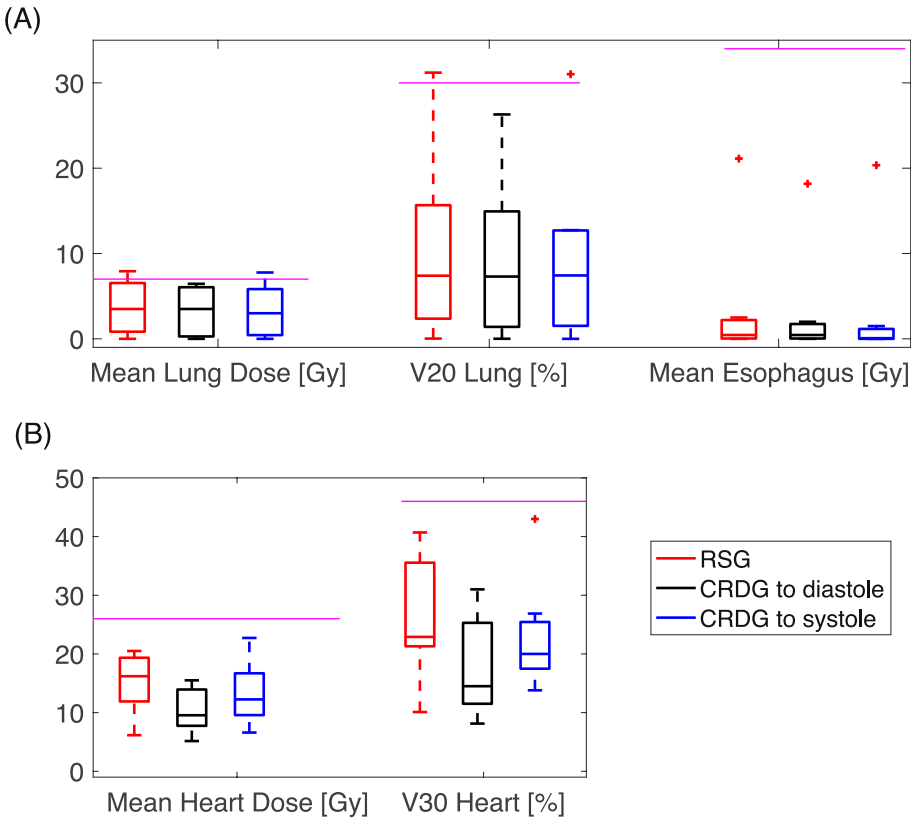

Fig. 2. Dose metric summary (Mean Dose (A) and Volume (B)) of RSG (red) and CRDG plans (black: CRDG phase to diastole, blue: to systole). The purple lines represent the dose constraints used in planning (also shown in Supplementary Material Table 2). The box contains medians and 25th and 75th percentiles. Whiskers are for maximum and minimum and outliers are presented as a marker (+). (For interpretation of the references to colour in this figure legend, the reader is referred to the web version of this article.)

OAR mean doses with respect to the field geometry. For 29 plans, there was a strong correlation between the dose homogeneity (D_5–D_{95}) and the beam range (p *less than 0*.003, Supplementary Material Fig. 3).

Regardless of which CRDG gating phase was used, there is a reduction in OAR mean doses for CRDG plans in general. Fig. 4 illustrates mean dose sparing of cardiac subsites between RSG and two CRDG plans for each cardiac target. The extent of OAR dose sparing varies with the location of the treatment target.

In the case where CRDG is most beneficial, exemplary DVHs are shown in Fig. 5A. In the case where CRDG is least beneficial, exemplary DVHs are shown in Fig. 5B. The mean ± SD dose reductions (%) were 28 ± 10 (heart at diastole), 21 ± 12 (heart at systole), 30 ± 17 (left ventricle at diastole) and 8 ± 9% (left ventricle at systole), presented in Table 1.

The residual motions (mm) when gated at diastole were 0.8 ± 0.5 with 20% duty cycle, 2.1 ± 1.0 (30%) and 2.7 ± 1.6 (40%), while when gated at systole were 1.9 ± 1.2 (20%), 2.0 ± 1.1 (30%) and 4.1 ± 2.6 (40%), respectively. The volume changes (%) when gated at diastole were −0.44 ± 2.9 (20%), 1.2 ± 7.2 (30%), and 1.2 ± 11.4 (40%), while when gated at systole were −0.1 ± 7.0 (20%), −0.9 ± 7.0 (30%), and 1.2 ± 15.0 (40%), respectively. The volume changes (cm^3) when gated at diastole were −0.5 ± 1.5 (20%), −0.5 ± 8.4 (30%), and −0.4 ± 8.7 (40%), while when gated at systole were 0.3 ± 6.9 (20%), −0.3 ± 6.9 (30%), and 2.9 ± 15.9 (40%), respectively. The target motion analysis is shown in Supplementary Material Table 5.

4. Discussion

In this study we investigated the OAR dose reduction with cardiac

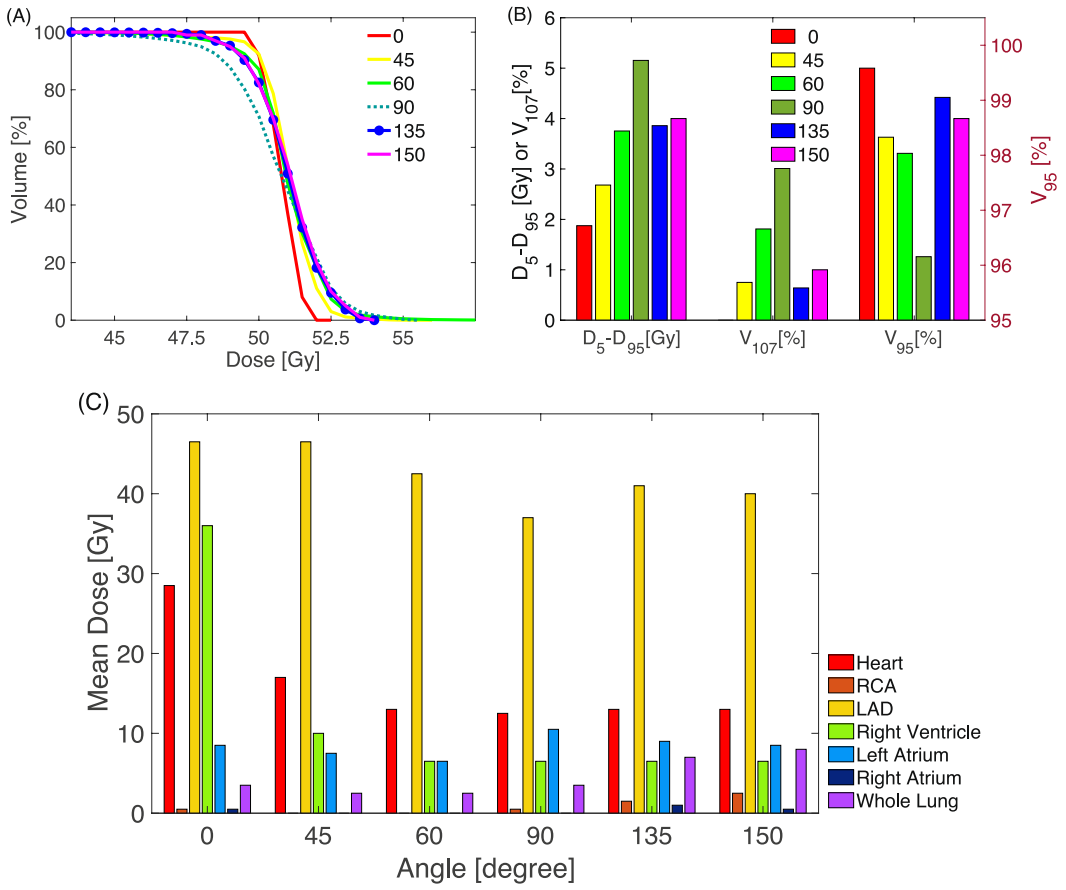

Fig. 3. Trade-off between the beam geometries. The target (PTV) is at left ventricular free wall. (A): Target coverage in DVH. (B): dose homogeneity (D_5–D_{95}), overdose (V_{107}) and dose coverage (V_{95}). D_5–D_{95} and V_{107} use the black label on the left y axis and V_{95} reads the red label on the right y axis). (C): OAR mean doses. (For interpretation of the references to colour in this figure legend, the reader is referred to the web version of this article.)

gating, particularly when cardiac targets are irradiated with cardiac and respiratory dual gating. Radiation treatment of a tumor on the heart is challenging due to the complexity of breathing and cardiac motions involved in targeting. The targets included ITVs throughout the whole cardiac cycle for respiratory single gating and were drawn at a gating phase for cardiac respiratory single gating. The dose differences in OARs were more prominent in cardiac subsites. The reductions (mean ± SD (%)) were 28 ± 10 (heart at diastole), 21 ± 12 (heart at systole), 30 ± 17 (left ventricle at diastole) and 8 ± 9% (left ventricle at systole).

The extent of cardiac OAR sparing by CRDG varied depending on how much dose the adjacent OARs received in the RSG plan. For example, Fig. 5A shows LAD and left ventricle received relatively high doses in the RSG plan for the target at left ventricular free wall. The LV mean dose was reduced by 14 Gy and heart mean dose by 6.5 Gy as shown in Fig. 4. Another example is Fig. 5B presenting RCA received the highest dose in the RSG plan for the target at right atrium free wall and the mean RCA dose was reduced by 8.3 Gy (Fig. 4).

However, in the case that the dose to the adjacent OARs was a concern, the benefit of CRDG may not be clinically meaningful. Also, the decision of an optimal beam geometry and cardiac gating phase is ultimately a balance between plan quality and clinical factors such as the patient's comorbidity.

The reported motion analysis indicates that the residual motions can be accounted for when multiple cardiac phases are used for gating. The optimal cardiac duty cycle has been investigated mostly in medical imaging including CT [25–29] and MRI [30]. The goal in these studies was to minimize residual motion (or motion artifacts) by finding a quiescent cardiac period to prospectively gate cardiac imaging [25], or an acquisition window for better reconstruction [26,27]. For cardiac imaging typically done with breath hold, a larger gating window (or duty cycle) will allow for a shorter breath hold period but will also compromise image quality [29]. Since the onset and duration of the optimum gating window highly depends on the subject's heart rate and inter-individual variability, the best approach is to investigate these parameters for each subject [28,30]. A few studies have been done for coronary arteries, suggesting that a 40% gating window [27] or reconstruction window on the order of 300 ms [26] results in the best image quality for diagnosis. However, in radiation therapy, longer duty cycles will require an internal target volume (ITV) to ensure displacement of the target centroid as well as volume change. No study to find the optimal cardiac gating window has been conducted particularly for radiotherapy. Our preliminary analysis is shown in Table VI, but the optimal duty cycle would require further investigation.

For the relationship between the homogeneity and range, the larger the range was, the worse the homogeneity, leading to less sharp distal dose falloff. We could speculate that as protons travel a path through more tissues, the beam energy gets more degraded due to increased effects of staggering and coulomb scattering.

Many researchers have been investigating possibilities of a non-invasive cardiac stereotactic radiosurgery for a non-oncological target, cardiac arrhythmia, with a radiotherapy equipped linear accelerator [11,14,31], carbon-ions [17], CyberKnife [12], and MRI-Linac [32]. Even with the recent demonstration of the short-term feasibility and efficacy of non-invasive cardiac stereotactic radiosurgery [14], potential long-term side effects such as inflammation and necrosis still remain a concern [31,32].

However, cardiac ablation treatment is different from cardiac sarcoma treatment in terms of the dose prescriptions, fractionation, the

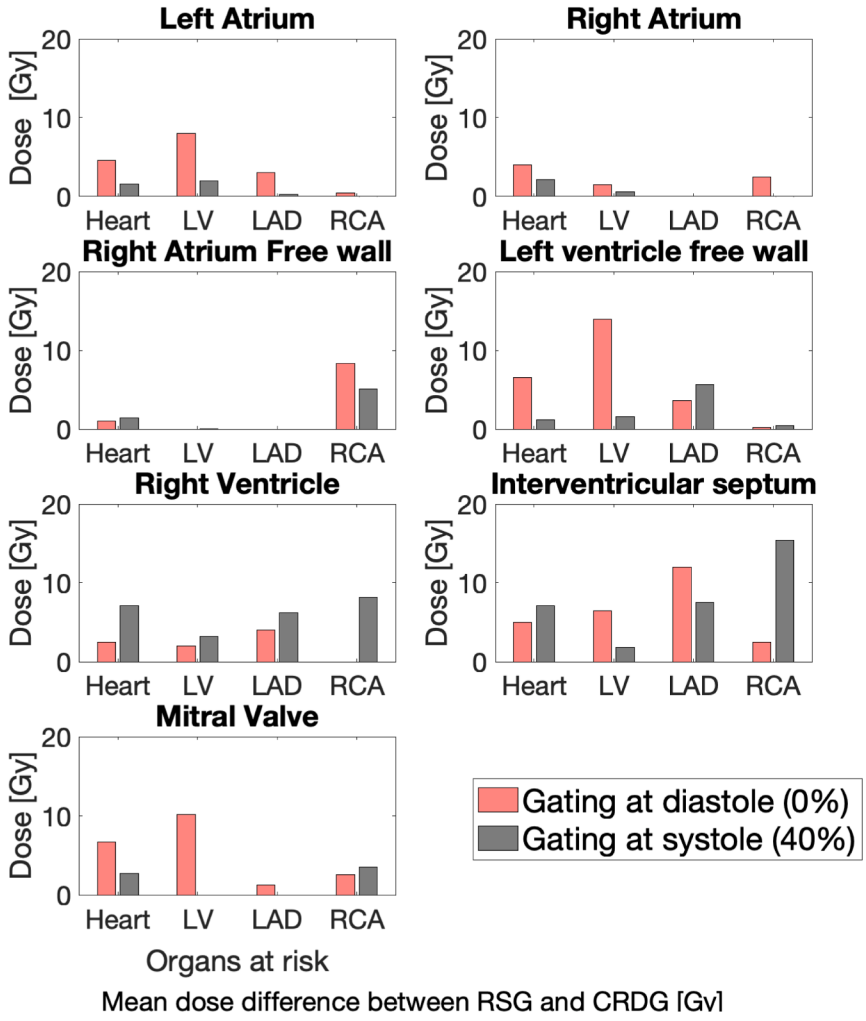

Fig. 4. Mean dose difference between RSG and CRDG for a target located at various cardiac substructures. The location is specified at the title of each subplot. Red bars show dose difference between RSG and CRDG phase at diastole (0%). Gray bars show dose difference between RSG and CRDG phase at systole (40%). (For interpretation of the references to colour in this figure legend, the reader is referred to the web version of this article.)

target volume, dose distribution in the target and the OAR constraints. The decision of an optimal beam geometry and cardiac gating phase is ultimately a balance between plan qualities and clinical factors such as the patient's comorbidity. In practice, a choice of 2–4 fields will be used for particle therapy to minimize the range uncertainty and increase the conformality. Cardiac ablation targets are likely also smaller, which requires a shorter extent of SOBP modulation. The increased proximal dose will be smaller than the conventional or sarcoma patients. But clearly, multiple beams provide a robust beam geometry for a motion and will spread out the entrance or proximal doses. The OAR dose reductions presented in this paper can be relevant to support cardiac ablations if cardiac gating is used, even when an appropriate selection of fields is used.

Imaging for treatment planning and motion assessment plays an important role in cardiac irradiation. As Graeff and Bert pointed out [33], the complex interplay between breathing and cardiac motion requires improved 5D image reconstruction, yet, these two motions can only be assessed separately until 5D image reconstruction becomes available. For accurate 4D dose optimization and accumulation, image registration between respiratory and cardiac 4D images might be necessary. Although deformable image registration (DIR) methods have been extensively evaluated for respiratory motions, DIR of the heart motion may require special attention or validation due to the large deformation of the heart muscles throughout the contractile motion. It is critical to evaluate the quality of DIR for cardiac sarcoma planning since it could compromise the mapping of voxels in tissue contours and introduce errors in 4-D dose accumulation. In this study, we used cardiac 4DCTs obtained at end of exhale for planning and dose accumulation, where doses to reference CTs were accumulated deformably using MIM [34] and the registrations were reviewed during the process.

This study has limitations. It is important to note that the number of cases included in this study was limited. However, from a clinical database of previously treated cardiac sarcoma patients at our institution, the average target motion (cm) throughout a cardiac cycle was 0.7 $\pm$ 0.7, while the average target motion (cm) in this study was 0.4 $\pm$ 0.5, summarized in Supplementary Material Table 6. We believe that the study data can be a good representative of our clinical experience.

We started studying the technical implementation of RSG and CRDG and their associated dosimetry planning for pencil beam scanning (PBS) beam deliveries. In particular, the interplay between the spot scanning and the target motion will be carefully studied and reported using the time-resolved simulation of beam deliveries with 4D Monte-Carlo simulation in future studies.

A technical implementation of dual-gated beam delivery to proton machines requires a careful study of various timing components of proton accelerator. The time delay and reproducibility of delivery between the actual cardiac motion and the beam on/off control play an important role in generating stable and clinically useful dose

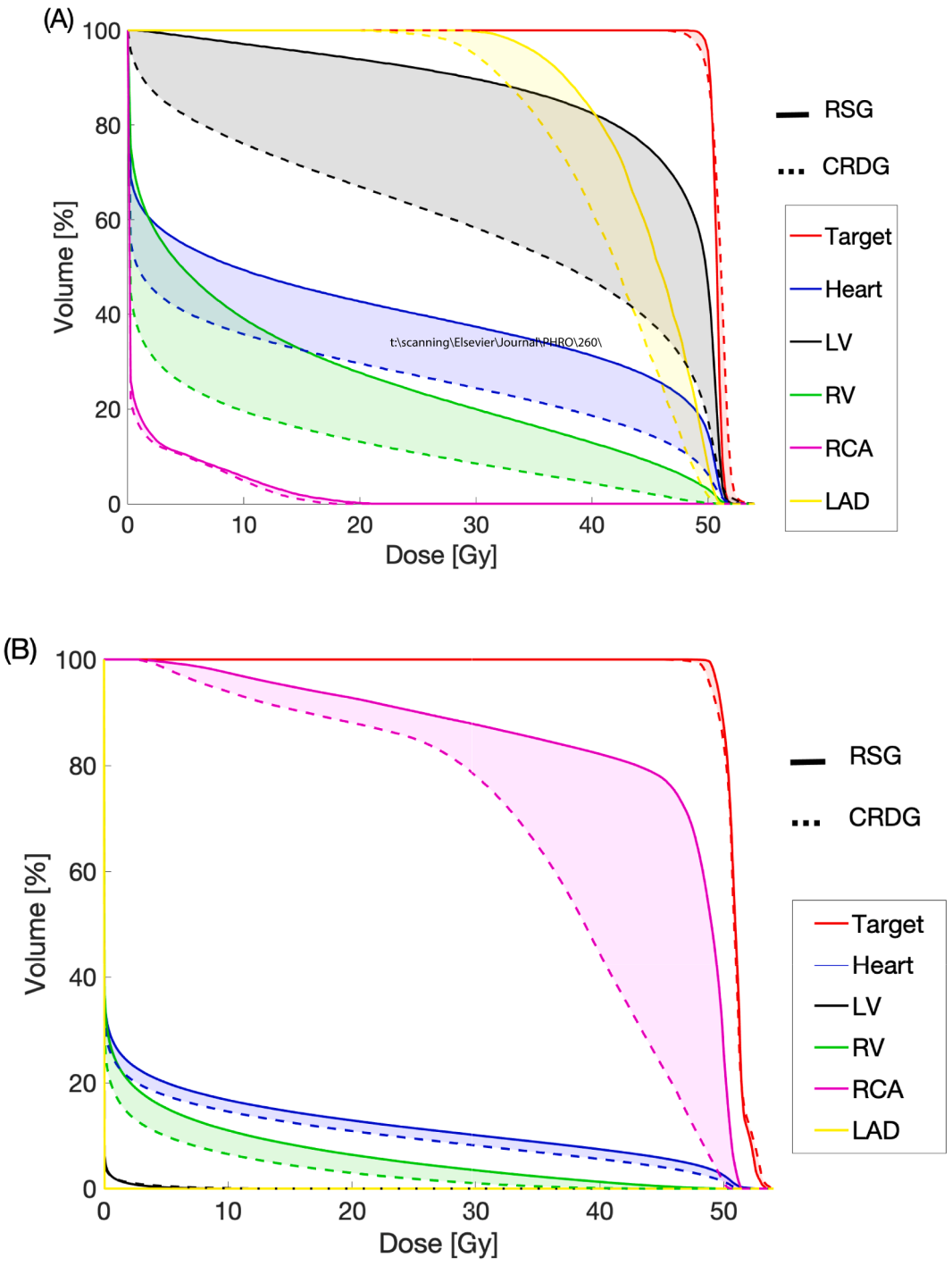

Fig. 5. RSG vs. CRDG (diastole) for a target located at (A) Left Ventricular Free Wall and (B) Right Atrial Free Wall. The reduced dose is shown as shaded. (LV: left ventricle, RA: right ventricle).

Table 1
Mean dose reductions in percentage for heart and left ventricle at each CRDG gating phase compared to RSG plans.

OAR	Target/ phase	Left Atrium	Left ventricular free wall	Right atrium	Right atrium free wall	Right ventricle	Interventricular septum	Mitral valve	Average ± SD
Heart	Diastole	35%	32%	35%	16%	14%	24%	41%	28 ± 10%
	Systole	12%	5%	19%	18%	39%	37%	18%	21 ± 12%
Left ventricle	Diastole	44%	31%	29%	0%	15%	36%	57%	30 ± 17%
	Systole	14%	4%	3%	0%	26%	11%	0%	8 ± 9%

distributions. An early investigation of the CRDG implementation to a proton machine has been made related to this work [35] and its results will be reported in a separate study.

In conclusion, we have demonstrated that CRDG can spare OARs better than RSG. Regardless of which cardiac gating phase was used, there was a reduction in OAR mean doses for CRDG plans.

Declaration of Competing Interest

The authors declare that they have no known competing financial interests or personal relationships that could have appeared to influence the work reported in this paper.

Acknowledgement

The authors thank Vince Kim for his help with proton beam planning and Dr. G. Chen for the initial development and support.

Funding

This work was supported by the Federal share of Project Income Program (project number 224001) at Massachusetts General Hospital.

Appendix A. Supplementary data

Supplementary data to this article can be found online at https://doi.org/10.1016/j.phro.2021.06.001.

References

[1] Hamidi M, Moody JS, Weigel TL, Kozak KR. Primary cardiac sarcoma. Ann. Thorac. Surg. 2010;90:176–81. https://doi.org/10.1016/j.athoracsur.2010.03.065.
[2] Butany J, Nair V, Naseemuddin A, Nair GM, Catton C, Yau T. Cardiac tumours: diagnosis and management. Lancet Oncol. 2005;6:219–28. https://doi.org/10.1016/S1470-2045(05)70093-0.
[3] Shanmugam G. Primary cardiac sarcoma. Eur. J. Cardiothorac. Surg. 2006;29:925–32. https://doi.org/10.1016/j.ejcts.2006.03.034.
[4] Randhawa JS, Budd GT, Randhawa M, Ahluwalia M, Jia X, Daw H, et al. Primary cardiac sarcoma: 25-year cleveland clinic experience. Am. J. Clin. Oncol. 2016;39:593–9. https://doi.org/10.1097/COC.0000000000000106.
[5] Wu Y, Million L, Moding EJ, Scott G, Berry M, Ganjoo KN. The impact of postoperative therapy on primary cardiac sarcoma. J. Thorac. Cardiovasc. Surg. 2018;156:2194–203. https://doi.org/10.1016/j.jtcvs.2018.04.127.
[6] Isambert N, Ray-Coquard I, Italiano A, Rios M, Kerbrat P, Gauthier M, et al. Primary cardiac sarcomas: a retrospective study of the French sarcoma group. Eur. J. Cancer 2014;50:128–36. https://doi.org/10.1016/j.ejca.2013.09.012.
[7] Thariat J, Clément-Colmou K, Vogin G, Beckendorf V, Ducassou A, Ali AM, et al. Irradiation des sarcomes cardiaques de l'adulte. Cancer Radiother. 18:125–31. doi: 10.1016/j.canrad.2014.02.003.
[8] Look Hong NJ, Pandalai PK, Hornick JL, Shekar PS, Harmon DC, Chen Y-L, et al. Cardiac angiosarcoma management and outcomes: 20-Year single-institution experience. Ann. Surg. Oncol. 2012;19:2707–15. https://doi.org/10.1245/s10434-012-2334-2.
[9] Aoka Y, Kamada T, Kawana M, Yamada Y, Nishikawa T, Kasanuki H, et al. Primary cardiac angiosarcoma treated with carbon-ion radiotherapy. Lancet Oncol. 2004;5:636–8. https://doi.org/10.1016/S1470-2045(04)01600-6.
[10] Keall PJ, Mageras GS, Balter JM, Emery RS, Forster KM, Jiang SB, et al. The management of respiratory motion in radiation oncology report of AAPM Task Group 76a): Respiratory motion in radiation oncology. Med. Phys. 2006;33:3874–900. https://doi.org/10.1118/1.2349696.
[11] Cuculich PS, Schill MR, Kashani R, Mutic S, Lang A, Cooper D, et al. Noninvasive cardiac radiation for ablation of ventricular tachycardia. N. Engl. J. Med. 2017;377:2325–36. https://doi.org/10.1056/NEJMoa1613773.
[12] Blanck O, Ipsen S, Chan MK, Bauer R, Kerl M, Hunold P, et al. Treatment Planning Considerations for Robotic Guided Cardiac Radiosurgery for Atrial Fibrillation. Muacevic A, Adler JR, editors. Cureus. Cureus; 2016;8:e705. doi: 10.7759/cureus.705.
[13] Eichhorn AV. In-Vivo Feasibility Study and Developments for Cardiac Arrhythmia Ablation using Scanned Carbon Ions [dissertation]. [Darmstadt]: Technische Universität Darmstadt; 2017.
[14] Cuculich P, Kashani R, Mutic S, Hallahan DE, Robinson CG. Myocardial performance after ep-guided noninvasive cardiac radioablation (ENCORE) for ventricular tachycardia (VT). Int. J. Radiat. Oncol. Biol. Phys. 2017;99:E511–2. https://doi.org/10.1016/j.ijrobp.2017.06.1827.
[15] Refaat MM, Ballout JA, Zakka P, Hotait M, Al Feghali KA, Gheida IA, et al. Swine atrioventricular node ablation using stereotactic radiosurgery: methods and in vivo feasibility investigation for catheter-free ablation of cardiac arrhythmias. J. Am. Heart Assoc. 2017;6:e007193. https://doi.org/10.1161/JAHA.117.007193.
[16] Richter D, Lehmann HI, Eichhorn A, Constantinescu AM, Kaderka R, Prall M, et al. ECG-based 4D-dose reconstruction of cardiac arrhythmia ablation with carbon ion beams: application in a porcine model. Phys. Med. Biol. 2017;62:6869. https://doi.org/10.1088/1361-6560/aa7b67.
[17] Lehmann HI, Graeff C, Simoniello P, Constantinescu A, Takami M, Lugenbiel P, et al. Feasibility study on cardiac arrhythmia ablation using high-energy heavy ion beams. Sci. Rep. 2016;6:38895. https://doi.org/10.1038/srep38895.
[18] Constantinescu AM. Planning studies for a non-invasive treatment of atrial fibrillation with scanned ion beams [dissertation]. [Darmstadt, Germany]: Technische Universität; 2014.
[19] Lu H-M, Brett R, Sharp G, Safai S, Jiang S, Flanz J, et al. A respiratory-gated treatment system for proton therapy. Med. Phys. 2007;34:3273–8. https://doi.org/10.1118/1.2756602.
[20] Chen Y-L. Proton Radiotherapy for Cardiac and Pulmonary Vessel Sarcomas. Particle Therapy Co-Operative Group. 2010.
[21] Hong L, Goitein M, Bucciolini M, Comiskey R, Gottschalk B, Rosenthal S, et al. A pencil beam algorithm for proton dose calculations. Phys. Med. Biol. 1996;41:1305–30. https://doi.org/10.1088/0031-9155/41/8/005.
[22] Gagliardi G, Constine LS, Moiseenko V, Correa C, Pierce LJ, Allen AM, et al. Radiation dose-volume effects in the heart. Int. J. Radiat. Oncol. 2010;76:S77–85. https://doi.org/10.1016/j.ijrobp.2009.04.093.
[23] Marks LB, Bentzen SM, Deasy JO, Kong F-M-S, Bradley JD, Vogelius IS, et al. Radiation dose-volume effects in the Lung. Int. J. Radiat. Oncol. 2010;76:S70–6. https://doi.org/10.1016/j.ijrobp.2009.06.091.
[24] Werner-Wasik M, Yorke E, Deasy J, Nam J, Marks LB. Radiation dose-volume effects in the esophagus. Int. J. Radiat. Oncol. 2010;76:S86–93. https://doi.org/10.1016/j.ijrobp.2009.05.070.
[25] Zamyatin A, Karbeyaz BU, Shaughnessy C, Rozas D. Optimal cardiac phase in prospectively gated axial cardiac CT scans. In: Lo JY, Schmidt TG, Chen G-H, editors. Medical Imaging 2018: Physics of Medical Imaging; Proceedings of SPIE, volume 10573; 2018 Feb 12-15; Houston, Texas, United States. Bellingham, Washington: SPIE; p. 931–8. doi: 10.1117/12.2293862.
[26] Celeng C, Vadvala H, Puchner S, Pursnani A, Sharma U, Kovacs A, et al. Defining the optimal systolic phase targets using absolute delay time for reconstructions in dual-source coronary CT angiography. Int. J. Cardiovasc. Imaging 2016;32:91–100. https://doi.org/10.1007/s10554-015-0755-2.
[27] Isma'eel H, Hamirani YS, Mehrinfar R, Mao S, Ahmadi N, Larijani V, et al. Optimal phase for coronary interpretations and correlation of ejection fraction using late-diastole and end-diastole imaging in cardiac computed tomography angiography: implications for prospective triggering. Int. J. Cardiovasc. Imaging 2009;25:739–49. https://doi.org/10.1007/s10554-009-9481-y.
[28] Hoffmann MHK, Lessick J, Manzke R, Schmid FT, Gershin E, Boll DT, et al. Automatic determination of minimal cardiac motion phases for computed tomography imaging: initial experience. Eur. Radiol. 2006;16:365–73. https://doi.org/10.1007/s00330-005-2849-z.
[29] Panetta D, Gabelloni M, Faggioni L, Pelosi G, Aringhieri G, Caramella D, et al. Cardiac computed tomography perfusion: contrast agents, challenges and emerging methodologies from preclinical research to the clinics. Acad. Radiol. 2021;28:e1–13. https://doi.org/10.1016/j.acra.2019.12.026.
[30] Scott AD, Keegan J, Firmin DN. Motion in cardiovascular MR imaging. Radiology 2009;250:331–51. https://doi.org/10.1148/radiol.2502071998.
[31] Zei Paul C, Maguire Patrick. Noninvasive ablation of ventricular tachycardia. N. Engl. J. Med. 2018;378:1650–2. https://doi.org/10.1056/NEJMc1802625.
[32] John RM, Stevenson WG. Noninvasive ablation of ventricular tachycardia. N. Engl. J. Med. 2017;377:2388–90. https://doi.org/10.1056/NEJMe1713245.
[33] Graeff C, Bert C. Noninvasive cardiac arrhythmia ablation with particle beams. Med. Phys. 2018;45:e1024–35. https://doi.org/10.1002/mp.12595.
[34] Piper J, Nelson A, Harper J. Deformable image registration in MiM Maestro Evaluation and Description. WhitePaper TD-473 [Internet]. Available from: https://s3.amazonaws.com/downloads.mimsoftware.com/Deformable_Image_Registration_in_MIM_Maestro_Evaluation_and_Description.pdf.
[35] Lee H, Jee K-W, Brett R, Chen Y-L, Pursley J, Flanz J, et al. Implementation of respiratory and cardiac double-gating to passive scattered proton delivery. Med. Phys. 2018;45:e666.